Nano Biomed Eng
2020, 12(1): 104-113. doi: 10.5101/nbe.v12i1.p104-113.

Research Article

Biological and Photocatalytic Activity of Silver Nanoparticle Synthesized from *Ehretia laevis* Roxb. Leaves Extract

Sudipata Panja[1], Indranil Choudhuri[1], Kalyani Khanra[1], BikasRanjan Pati[2], Nandan Bhattacharyya[1]
[1]Department of Biotechnology, Panskura Banamali College, P.O. - Panskura R.S., Dist. - Purba Medinipur, West Bengal, PIN 721152, India.
[2]Department of Microbiology, Vidyasagar University, Rangamati, Medinipur, West Bengal, PIN 721102, India.

Corresponding author. E-mail: bhattacharyya_nandan@rediffmail.com

Received: Jan. 7, 2020; **Accepted:** Mar. 25, 2020; **Published:** Mar. 25, 2020.

Citation: Sudipata Panja, Indranil Choudhuri, Kalyani Khanra, BikasRanjan Pati, and Nandan Bhattacharyya, Biological and Photocatalytic Activity of Silver Nanoparticle Synthesized from *Ehretia laevis* Roxb. Leaves Extract. *Nano Biomed. Eng.*, 2020, 12(1): 104-113.
DOI: 10.5101/nbe.v12i1.p104-113.

Abstract

Silver nanoparticles were synthesized from *Ehretia laevis* Roxb. leaf extract by one-step green synthesis method. The nanoparticles were crystalline in nature, spherical shaped with 25 to 35 nm diameter. The aim of this study was the synthesis and characterization of silver nanoparticles from *Ehretia laevis* Roxb., and the evaluation of their antimicrobial, anticancer, larvicidal and methylene blue dye degradation efficiency. The nanoparticles showed antimicrobial, larvicidal and cytotoxic activity. At a concentration of 25 µg/mL, it killed 70 ± 10.24% of *Culex quinquefasciatus* larvae after 72 h treatment. The median lethal concentration of the nanoparticles against HeLa, human cervical cancer cells, and MCF-7 human breast cancer cells, were calculated to 12.7 µg/mL and 14.5 µg/mL, respectively. The synthesized nanoparticles degraded Congo red ~ 85% within 8 h at a concentration of 200 µg/mL. Possible application of the synthesized nanoparticles are water purifying agent in presence of sunlight.

Keywords: Antimicrobial activity; Cytotoxicity; *Ehretia laevis* Roxb.; Photocatalytic activity; Silver nanoparticles

Introduction

Nanomaterials possess enhanced physicochemical properties and biological activities in comparison with the bulk materials. This property makes nanoparticles useful in different fields of science and technology [1-11]. Researchers emphasize on silver nanoparticles because of its opportunity in the field of high information storage, electroluminescence and photoluminescence devices [12]. Silver nanoparticles are also used in preparation of medical devices, drinking water purification, cosmetics, textile industry and as disinfection agents [13].

Textile effluents contain organic dyes, which is highly stable in light and washing. Those dyes are very toxic and cannot be easily degraded by conventional biological and chemical treatments. The application of nanoparticles in the photocatalytic degradation of pollutants in wastewater is more effective than the conventional method due to rapid oxidation of pollutant and no byproduct of polycyclic compounds [14]. Nanoparticles having antimicrobial, larvicidal and photocatalytic activity might be useful to remove contaminants from effluent water [15].

Green synthesis of silver nanoparticles is preferable than the traditional physical or chemical process, because it is inexpensive, eco-friendly, one-step process, and can be synthesized without costly instruments and produce less hazards [16]. Previous studies used fungus [17], bacteria [18], algae [19], and medicinal plant extracts [20-25] as reducing and capping agents for the synthesis of silver nanoparticles. In case of plant tissues, leaves are a good source of phytochemicals which may be used as reducing as well as stabilizing agents for the synthesis of silver nanoparticles, although root, stem bark, leaf, fruit and flower extracts were also used for the synthesis of silver nanoparticle.

Ehretia laevis Roxb. (*E. laevis* Roxb.) is generally a shrub, may be up to 12 m in height, commonly found in the deciduous and monsoonal forests. The bark, leaves and fruit of this plant are edible. The leaf extracts of *E. laevis* Roxb. is a good source of phenolic compounds, traditionally used in the treatment of dysentery, eczema, intestinal worms and to cure wounds. A significant quantity of tannin is found in the stem bark, and the fruit is enriched with vitamin C and flavonoids. The root and stem bark extract are used for the treatment of syphilis and diphtheria [26, 27]. In this study, silver nanoparticles were synthesized from leaf extract of *E. laevis* (El Ag NP) by one-step green synthesis method, and their antimicrobial, larvicidal, cytotoxic, and photocatalytic activities are evaluated for possible applications.

Experimental

Plant materials

The leaves of *E. laevis* were collected from *Amlachati*, Pashchim Medinipur, West Bengal, India (22°22'36" N, 87°02'36" E), during summer. The plant was identified by the experts of *Ex-situ* conservation site of Medicinal plant species, *Amlachati*, West Bengal, India.

Synthesis of silver nanoparticles

The plant leaves were cleaned thoroughly with distilled water and air dried. Aqueous leaf extract was prepared by boiling the mechanically chopped leaves in deionized water (10 : 1 v/w) at 80 °C for 1 h, and filtrated through 0.6 µm Whatman filter paper. 1 mM $AgNO_3$ was mixed with the aqueous leaf extracts in 1 : 9 v/v ratio and incubated at 90 °C for 1 h [28]. Synthesis of the silver nanoparticles (El Ag NPs) was confirmed by the colour change from light to deep brown [29]. Finally, colloidal suspension of the El Ag NPs was centrifuged at 8000 rpm in Remi R-247M rotor for 30 min to remove impurities [30, 31]. The pellet was re-suspended in sterile distilled water, and the previous step was repeated to wash the synthesized El Ag NPs [32, 33] for several times.

Characterization of the synthesized silver nanoparticles

The colour changes due to the reduction of Ag^+ were recorded by ultraviolet–visible (UV-Vis) spectrum [32, 34]. 1 mg sample was dissolved in 500 µL of deionised water, and spectrum recorded from 300 nm to 800 nm with a 1 nm resolution by using UV-Vis spectrophotometer (Eppendorf Bio Spectrometer). The particle size, shape and surface morphology of the synthesized El Ag NPs were studied by transmission electron microscopy (TEM) [35]. Aqueous solution of the synthesized nanoparticles was dropped on a carbon coated copper grids and allowed to dry. Excess solution was removed by using tissue paper. For this study, JEM-1200EX electron microscope (JEOL, Tokyo, Japan) was used and operated at an accelerating voltage of 120 kV. More than 150 particle sizes were analyzed to obtain the size distribution of the synthesized El Ag NPs. The chemical analysis of the synthesized El Ag NPs was studied by energy-dispersive X-ray spectroscopy analysis (EDX). The size distribution and potential stability in colloidal suspension of the synthesized AgNPs were studied by dynamic light scattering (DLS) and zeta potential respectively [36, 37]. For DLS and zeta potential the sample was prepared by diluting the nanoparticles 10 times in 150 mM phosphate buffered saline (PBS) of pH 7.4 and measured by MALVERN Zeta Sizer Nano ZS. The face center cubic crystalline nature of the synthesized Ag NPs was studied by X-ray powder diffraction (XRD). XRD was conducted by X'pert-pro X-ray diffractometer at voltage 40 kV and current of 30 mA in 2θ angle pattern. Copper K-α radiation was used to recorded the spectrum in the range of 20° to 100° [15, 28, 37]. Fourier transform infrared spectroscopy (FTIR) was used to classify the biomolecules in leaf extract of *E. laevis* involved in the reduction of metal ion and stabilizing the synthesized nanoparticles. Dry powder of El Ag NPs was mixed with KBr, and FTIR analysis was performed by Perkin-Elmer Spectrometer FTIR Spectrum Two in the range of 4000 to 400 cm^{-1} with a resolution of 1 cm^{-1} [37].

Antimicrobial activity study

Human pathogenic gram-positive bacteria like *Bacillus subtilis, Enterococcus faecalis, g*ram-negative bacteria such as *Pseudomonas aeruginosa, Escherichia coli* were used to study the antimicrobial activity of the synthesized El Ag NPs. Ciprofloxacin was used as a standard antibiotic. 4 different concentrations of El Ag NPs and ciprofloxacin (25-150 µg/mL) were used. The antimicrobial activity was studied by well diffusion method [35, 38]. 200 µL overnight grown cultures of each microbial strain (1×10^5 CFU/mL) were used to prepare lawns on Luria-Bertani agar plates. Sterilized stainless-steel cork borer of 6 mm diameter was used to prepare the well on the agar plates, and each well was loaded with 50 µL of different concentrations of Ag NPs and ciprofloxacin. The bacterial plates were incubated at 37 °C for 18 h. Antibiotic zone scale (Himedia, India) was used to measure the zone of inhibition. The mean value of the triplicate of the experiment was expressed in millimeter unit.

The minimum inhibitory concentration (MIC) is the concentration of the nanoparticle that completely inhibits the visible growth. In 5 mL of LB broth, the inoculum was added and incubated for 24 h at 37 °C in presence of different concentrations of El Ag NPs. Next-day growth was measured using spectrophotometer.

Larvicidal activity study

Third instar mosquito larvae of *Culex quinquefasciatus* was used to study the larvicidal activity of the synthesized nanoparticles [39, 40]. 20 mL aqueous solution of El Ag NPs was taken in 4 different petri plates at 2.5-25 µg/mL of concentrations, and triple distilled water was taken as control. 10 healthy and freshly washed larvae were kept into each plate at room temperature for 72 h, and dead larvae were counted manually.

% Mortality = [(% test mortality - % control mortality) / (100 - % control mortality)] × 100 [41].

Cytotoxicity study

Cytotoxicity of the synthesized El Ag NPs was evaluated by 3-(4,5-dimethylthiazol-2-yl)-2,5-diphenyl-tetrazolium bromide (MTT) assay. HeLa, MCF7 and HEK-293 cells were seeded in 96 wells tissue culture plates containing Dulbecco's modified Eagle medium (DMEM), 1% penicillin-streptomycin, and 10% fetal bovine serum (FBS), pH 7.2. The cells were incubated at 37 °C in presence of 5% CO_2 for 24 h [28]. Then the cells were treated with different doses of 1 - 25 µg/mL El Ag NPs solution. After overnight incubation, 0.5 mg/mL MTT in PBS was added into each well and incubated at 37 °C for 3.5 h, followed by 100 µL of DMSO being added into each well to dissolve the water insoluble formazan, and mixed by low speed shaking for 10 min. The colour changes were recorded using ELISA reader at 570 nm (Robonik, Readwell touch ELISA PLATE analyzer, India) against non-treated cells as control [15, 28, 32, 35]. The rate of survival of the cells is expressed as follows,

Cell viability (%) = $(OD_t / OD_c) \times 100$,

where OD_C = absorbency of control cells, and OD_t = absorbency of treated cells.

Photocatalytic activity of the synthesized Ag NPs

Methylene blue (MB) was used to study the photocatalytic activity of the synthesized El Ag NPs in presence of sunlight. Typically, 10 µg/mL solution of the dye was prepared in deionized water. Then, synthesized El Ag NPs were added to the dye solution by maintaining 200 µg/mL concentrations. To prepare a homogeneous suspension of the dye and El Ag NPs, the mixture was stirred for 0.5 h in darkness. Then, the dye solution was exposed to 400 W sodium vapor lamp at a distance of ~ 20 cm with constant stirring. A solution with the same concentration of MB dye without nanoparticle was kept under the same conditions, used as control. The ambient temperature was around 27±2 °C. After every 1 h, 1 mL suspension of the dye and El Ag NPs were taken and centrifuged at 4000 rpm for 10 min. The clear solutions of the dye were scanned in the range of 350 - 800 nm using UV-Vis spectrophotometer (Eppendorf Bio Spectrometer). The concentration of dye is directly proportional to the absorbance in the UV-Vis spectrophotometer [42]. The percentage of dye degradation was calculated by the following equation [43]:

% degradation = $(C_0\text{-}C)/C_0 \times 100$.

Here, C_0 is the initial dye concentration and C is the concentration of the dye after photocatalytic degradation.

The amount of MB degraded at equilibrium was calculated by following equation:

$q_t = [(C_0 - C_t) \times V] / m$,

where C_0 and Ct are the initial and final concentrations of dye in mg/L respectively. q_t is the amount of MB

dye degraded. V is the volume of MB dye in mL, and m is the initial mass of nanoparticles.

Pseudo first order and second order were the two models used to study the kinetics of photocatalytic degradation. The equation of pseudo first order kinetics was:

$\ln (q_e - q_t) = \ln q_e - kt$,

where q_e and q_t are absorption capacity at equilibrium and time t respectively, and k is the pseudo first order rate constant.

The equitation of second order model is:

$t/q_t = t / (K_2 q_{e2}) + t / q_e$,

where at time t, q_t is the amount of dye absorption and K_2 is pseudo second order rate constant.

Statistical analysis

All the experiments of the present study were performed in triplet, and data of the experiments were expressed in mean ± SD. Variance <5% (i.e. $p < 0.05$) was accepted as positive result.

Result and Discussion

Synthesis of silver nanoparticles

Plant extracts consist a variety of organic compounds. During the synthesis of silver nanoparticles, these compounds act as capping and reducing agents [33]. This change could be recorded by ultraviolet–visible spectroscopy (UV-Vis). Free electrons of metal nanoparticles yielded a surface plasmon resonance (SPR) absorption band [34]. For silver nanoparticles, a sharp band was found around 420 - 440 nm [44]. Fig. 1(b) shows a peak at 438 nm, which confirmed the presence of silver nanoparticles in solution.

The maximum yield of the synthesized El Ag NPs was obtained at the following conditions: Concentration of $AgNO_3$ was 3 mM, synthesis time was 60 min, and synthesis temperature was 90 °C (Fig. 2).

Characterization of synthesized nanoparticles

The synthesized nanoparticles were spherical

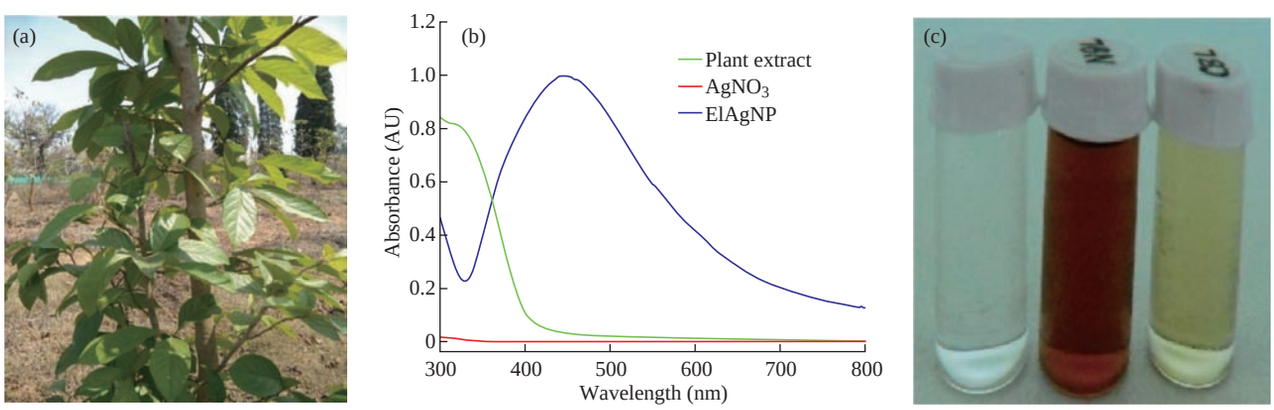

Fig. 1 **(a)** Whole plant of *Ehretia laevis* Roxb. **(b)** Absorption band of synthesized nanoparticles appeared at 438 nm. **(c)** Left, 1 mM/L silver nitrate solution; middle, silver nanoparticles synthesized from leaf extract of *E. laevis* Roxb.; right, leaf extract of *E. laevis* Roxb.

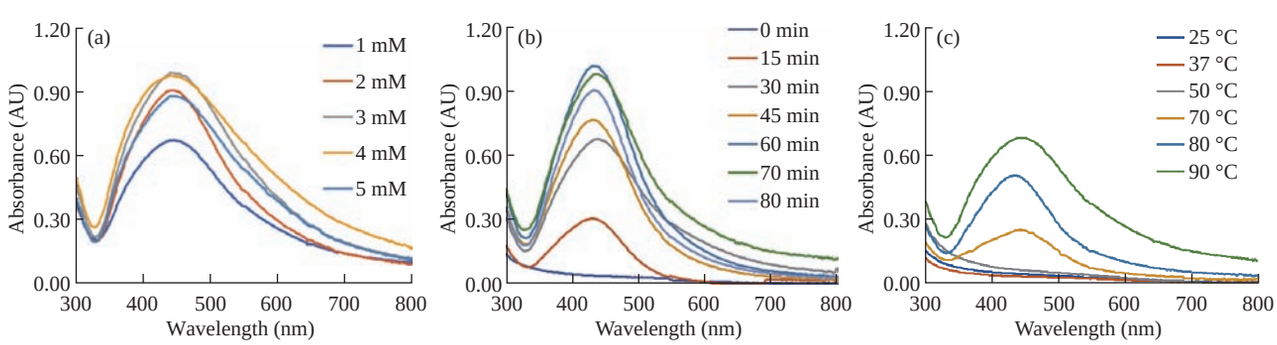

Fig. 2 Synthesis of silver nanoparticles in different conditions: **(a)** At different $AgNO_3$ concentrations; **(b)** at different time; and **(c)** at different temperatures.

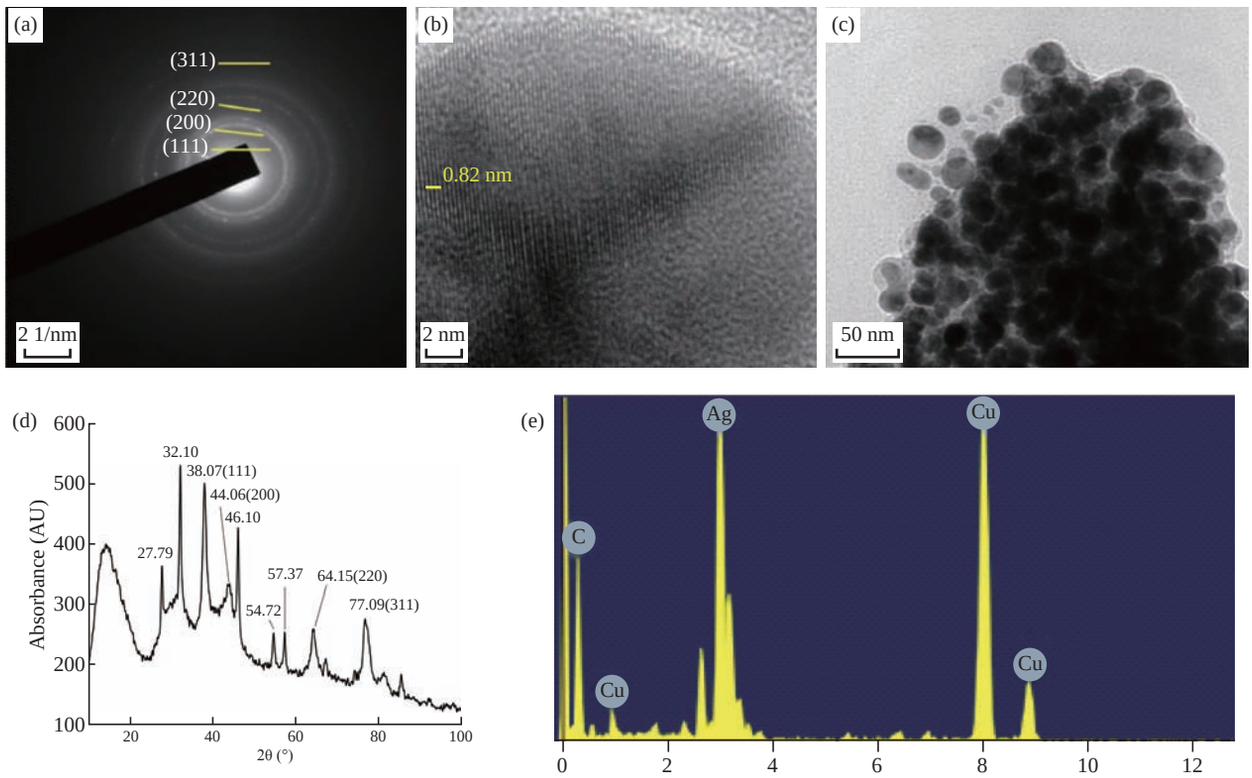

Fig. 3 Characterization of synthesized nanoparticles. **(a)** Selected area electron diffraction pattern; **(b)** scale bar 2 nm; **(c)** transmission electron microscopy images of the synthesized AgNPs, scale bar 50 nm; **(d)** X-ray diffraction pattern of El Ag NPs; **(e)** energy-dispersive X-ray spectroscopy confirmed the presence of silver in synthesized nanoparticles.

in shape having diameter 25 - 35 nm. The internal spacing between the 2 planes was approximately 0.273 nm, and there were approximately 146 planes present (Fig 3(b)). Some amount of synthesized Ag NPs was partially aggregated, but the non-aggregated was uniform in shape and size. Fig 3(a) represented selected area electron diffraction pattern of the El Ag NPs. The polycrystalline diffraction ring could be indexed at 111, 200, 220 and 311 nm, which indicated the shape of the synthesized El Ag NPs was face center cubic crystalline structure.

The crystalline nature of the synthesized El Ag NPs was confirmed by X-ray powder diffraction (XRD) analysis. 4 major peaks were observed in this spectrum. The distinct diffraction peaks at 2θ values of 38.07, 44.06, 64.15 and 77.09 could be indexed to the (111), (200), (220) and (311) reflection planes of face centered cubic structure of silver. This XRD pattern clearly showed the synthesis of silver nanoparticles from *E. laevis* Roxb. (JCPDS FILE No 04-0783) (Fig. 3(d)). Previous studies also reported the same type of peaks during the synthesis of silver nanoparticles [45, 46].

The elementary composition of the nanoparticles was studied by energy-dispersive X-ray spectroscopy (EDX). A strong signal at 3 KeV region [45] indicated the synthesis of Ag NPs from leaf extract of *E. laevis*. The spectrum also showed the presence of copper and carbon which might came from plant extract.

FTIR analysis confirmed the presence of different functional groups in the synthesized El Ag NPs.

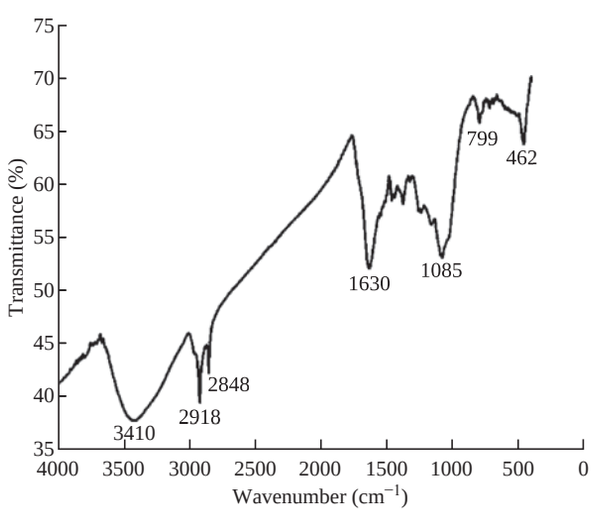

Fig. 4 Fourier-transform infrared spectrum of silver nanoparticles synthesized from *E. laevis*.

These functional groups acted as reducing agent for the reduction of Ag^{+} ion [33]. In this FTIR spectrum, major peaks were observed at 3410, 2918, 2848, 1630, 1085, 799 and 462 cm^{-1}. The sharp peak at 3410 cm^{-1} represented the O-H bond stretch or H bonding, and the functional group may be alcohol or phenol. The C-H stretch in alkenes was represented by peaks at 2918 and 2848 cm^{-1}. The peak at 1630 cm^{-1} indicated the presence of N-H band in 1^{0} amines. The peak at 1085 cm^{-1} indicated the presence of C-N stretch in aliphatic amines or the presence of =C-H bend in alkanes. The peaks at 799 and 462 cm^{-1} indicated the presence of alkyl halides in the synthesized nanoparticles [33].

Dynamic light scattering (DLS) is a technique used to study the size distribution profile in the suspension. The size of the nanoparticles is ranging between 24 to 43 nm, with an average size of 25 nm (Fig. 5(a)). This result justified the TEM result, and also indicated if the temperature of synthesis and concentration of leaf varied, then the shape and structure of the nanoparticle would vary [37]. The value of zeta potential is related to the short- and long-term stability of emulsions. Emulsions with high zeta potential (negative or positive) were electrically stabilized while emulsions with low zeta potentials tended to coagulate or flocculate [47]. Synthesized Ag NPs from leaf extract of *E. laevis* had a zeta value of 65 ± 5 mV and the El Ag NPs were highly stable in emulsion (Fig 5(b)).

Antimicrobial activity

Both gram-positive and gram-negative bacteria showed some sensitivity against the synthesized nanoparticles. At low concentration (25 µg/mL), *P. aeruginosa* (8.23 ± 0.84 mm) and *B. subtilis* (8.26 ± 1.5 mm) showed less zone of inhibition (ZOI) than *E. coli* and *E. faecatis* (10.33 ± 0.54 mm). With the increase of the concentration of El Ag NPs, the zone of inhibition also increased in linear pattern (Fig. 6). In comparison with ciprofloxacin, the nanoparticles showed less activity.

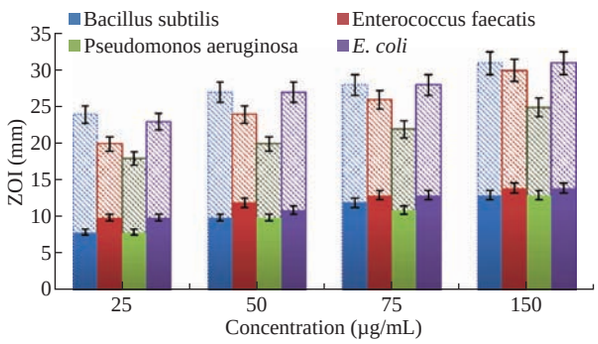

Fig. 6 The graphical presentation of zone of inhibition for bacterial species against synthesized El Ag NPs (solid fill) and ciprofloxacin (light color fill) at different concentrations.

The MIC value of the nanoparticles for *Enterococcus faecatis* was 255 µg/mL, 260 µg/mL for *Escherichia coli*, 230 µg/mL for *Pseudomonos aeruginosa*, and 230 µg/mL for *Bacillus subtilisis*. For *Aspergillus niger* and *Candida albicans*, the MIC value was 290 µg/mL and 315 µg/mL respectively.

Larvicidal activity

Larvicidal activity of the synthesized nanoparticles was studied in dose dependent manner against *C. quinquefasciatus* (Fig. 7). Aqueous plant extract of

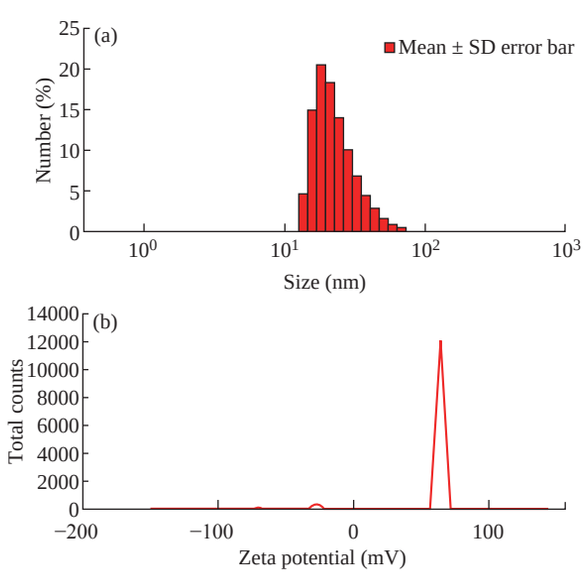

Fig. 5 **(a)** Dynamic light scattering and **(b)** zeta potential (mV) of the synthesized El Ag NPs.

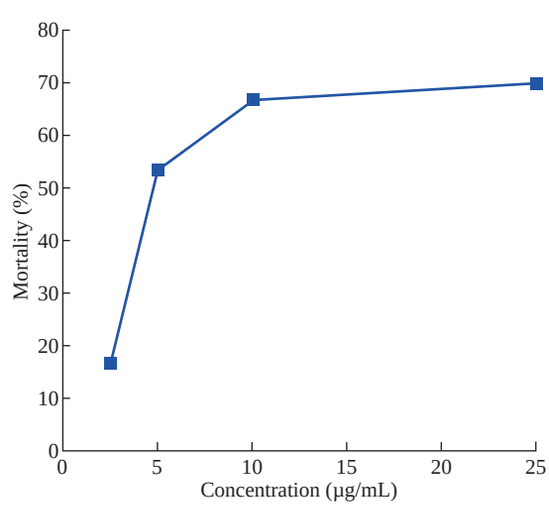

Fig. 7 Graphical representation of larvicidal activity of the synthesized nanoparticles at 72 h, data presented as mean ± SD of 3 individual experiments.

*E. laevis*shows showed not more than 7.2 ± 6.1% mortality, and 1 mM silver nitrate solution showed 10.7 ± 11.1% mortality after 72 h of incubation. At the same incubation time, 2.5 µg/mL concentration of El Ag NPs showed 16.7 ± 10.5% mortality, 5 µg/mL showed 53.3 ± 18.4% of mortality, 10 µg/mL showed 66.7 ± 11.4% of mortality. At the concentration of 25 µg/ml of ElAgNPs showed 70 ± 10.2% of mortality of mosquito larvae. The mortality was not significantly increased upon a concentration of 10 µg/mL El Ag NPs. At high concentration of El Ag NPs, the mosquito larvae may go to diapause stage [48].

Cytotoxicity assay

El Ag NPs possess toxicity against both HeLa and MCF-7 cells in dose dependent manner. MCF-7 is a breast cancer cell line slightly more sensitive than the HeLa which is a cervical cancer cell line. The HeLa cell line showed the biphasic behavior at 1 µg/mL of concentration of El Ag NPs. HeLa showed a rate of survival of 110.2%, while at the same concentration, MCF showed a survival rate of 783.7%. The LC_{50} as found for MCF-7 and HeLa cells were 14.5 and 12.7 µg/mL respectively. Previous literature showed the LC_{50} value of cisplatin for HeLa and MCF-7 was 13 and 55.8 µM respectively [49, 50]. At a concentration of 25 µg/mL of El Ag NPs, 67.4% population of MCF-7 and 54.8% population of HeLa cells were killed (Fig. 8). The nanoparticles were found to be more toxic to human embryonic kidney (HEK-293) cells. The LC_{50} as found for HEK-293 cells was 2.44 µg/mL.

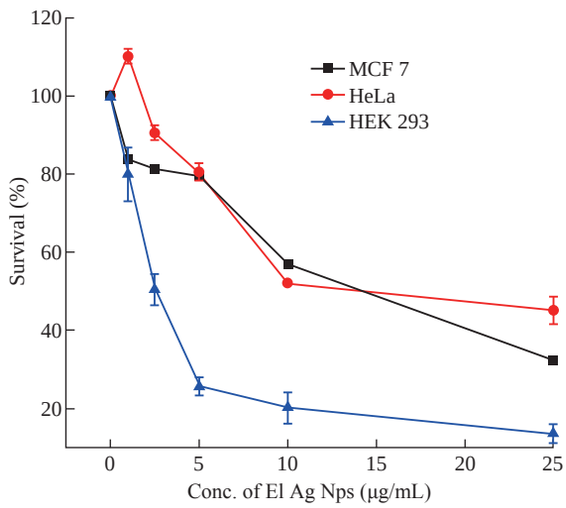

Fig. 8 Graphical representation of rate of survival of MCF-7, HeLa, and HEK 293 cells at different El Ag NPs concentrations, error bars indicating standard deviation of three individual experiments (n = 3).

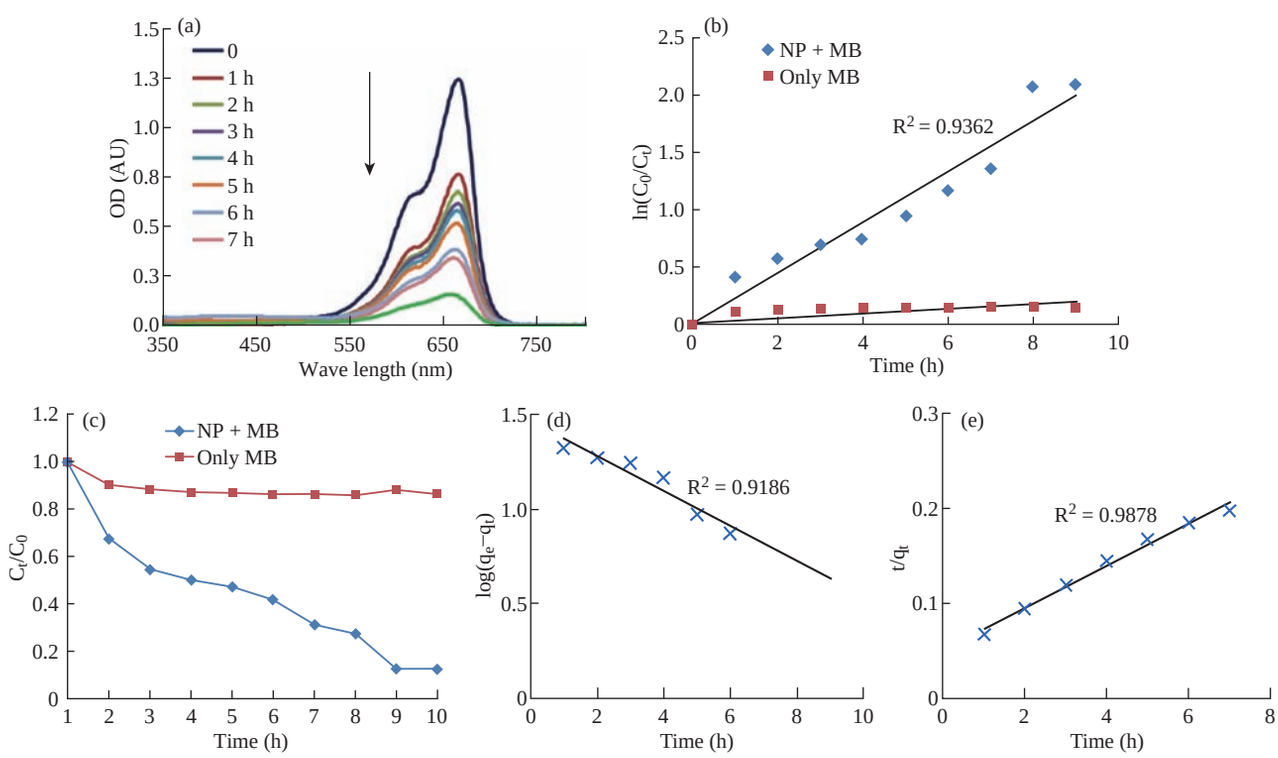

Fig. 9 **(a)** UV spectra showed methylene blue degradation activity of the nanoparticles in presence of light. **(b)** Kinetic fit plot of ln (C_0/C_t) vs time in case of methylene blue (MB) and nanoparticles (NPs) in presence of light. Here C_0 was initial dye concentration and C_t was the concentration of dye at time t. **(c)** Degradation of only methylene blue (MB) and methylene blue in presence of nanoparticles (NP + MB). **(d)** and **(e)** Pseudo first order and second order models of photocatalytic activity respectively.

Photocatalytic activity

The photoactinic activity of the synthesized El Ag NPs was studied against methylene blue dye solution in presence of light. The characteristic absorption pick was observed around 660 nm and the peak decreased with respect to the time of exposure (Fig. 9(a)). The synthesized nanoparticles degraded ~ 38% of dye in 1 h, and ~ 50% of dye in 3 h of exposure. After 8h, almost 88% dye was degraded. Fig. 9(b) shows the photo degradation in presence of nanoparticles which acted as photocatalyst. The degradation rate of MB in presence of only light was smaller than the degradation rate of MB in presence of both light and nanoparticles (Fig. 9(c)).

In case of pseudo first order model, the correlation coefficient value (R^2) 0.9186 representing the model was not good fit (Fig. 9(d)). The t/q_t vs time plot presented a linear plot with high correlation coefficient value 0.9878. This value was very closed to 1 (Fig. 9(e)), and so the bleaching of MB in presence of El Ag NPs followed the pseudo second order kinetics.

Conclusions

In conclusion, synthesized nanoparticles from the extract of *E. laevis* Roxb. leaves, were spherical in shape and fairly small in size. The nanoparticles were highly stable in solution and active in nature. It possessed biological activities like cytotoxicity, larvicidalactivity, and antimicrobial activity in some extend. The synthesized nanoparticles presented photocatalytic activity in presence of light. The kinetic model for methylene blue degration in presence of nanoparticles and light was established at pseudo second order kinetics. The nanoparticles were synthesized by green synthesis method which made them inexpensive and less hazardous. Methylene blue was widely used in industry and found in industrial effluents. The above mentioned characters of the synthesized nanoparticles indicated their possible applications in industrial waste water treatment.

Acknowledgements

Author is grateful to DBT-BOOST (Govt. of West Bengal) and DST-FIST (Govt. of India) for instrumentation support.

Conflict of Interests

The authors declare that no competing interest exists.

References

[1] T.M. Tolaymat, A.M. El Badawy, A. Genaidy, et al., An evidence-based environmental perspective of manufactured silver nanoparticle in syntheses and applications: A systematic review and critical appraisal of peer-reviewed scientific papers. *Science of the Total Environment*, 2010, 408(5): 999-1006.

[2] M. Gajendiran, H. Jo, K. Kim, et al., Green synthesis of multifunctional Peg-carboxylate π back-bonded gold nanoconjugates for breast cancer treatment. *Int J Nanomedicine*, 2019, 14: 819-834.

[3] S.O. Hasson, M.J. Al-Awady, M.J. Kadhim, et al., Silver nanoparticles as an effective anti-nanobacterial system towards biofilm forming pseudomonas oryzihabitans. *Nano Biomed. Eng*, 2019, 11(3): 297-305.

[4] K. Reena, M. Prabakaran, B. Leeba, et al., Green synthesis of pectin-gold-PLA-PEG-PLA nanoconjugates: In vitro cytotoxicity and anti-inflammatory activity. *Journal of Nanoscience and Nanotechnology*, 17 (7): 4549-4557.

[5] K. Reena, P. Balashanmugam, M. Gajendiran, et al., Synthesis of leucas aspera extract loaded Gold-PLA-PEG-PLA amphiphilic copolymer nanoconjugates: In vitro cytotoxicity and anti-inflammatory activity studies. *Journal of Nanoscience and Nanotechnology*, 16(5): 4762-4770.

[6] S.O. Hasson, M.J. Al-Awady, M.J. Kadhim, et al., Silver nanoparticles as an effective anti-nanobacterial system towards biofilm forming pseudomonas oryzihabitans. *Nano Biomed. Eng*, 2019, 11(3), 297-305.

[7] M. Gajendiran, P. Balashanmugam, P.T. Kalaichelvan, et al., Multi-drug delivery of tuberculosis drugs by π-back bonded gold nanoparticles with multiblockcopolyesters. *Materials Research Express*, 3(6): 065401.

[8] M. Prabakaran, V. Kalaiarasi, P. Nithya, et al., Green synthesis of piperine/triton X-100/silver nanoconjugates: Antimicrobial activity and cytotoxicity. *Nano Biomedicine and Engineering*, 2018, 10(2): 141-148.

[9] M. Prabakaran, P. Nithya, V. Kalaiarasi, et al., Green synthesis of piperine loaded gold/triton X-100 nanoconjugates: In-vitro evaluation of biocompatibility and anti-oxidant activity. *Nano Biomedicine and Engineering*, 2019, 11(2): 192-199.

[10] K Rajendran, M Gajendiran, S Kim, et al., Synthesis and characterization of biocompatible zinc oxide nanorod doped-titanium dioxide nanosheet. *Journal of Industrial and Engineering Chemistry*, 57: 387-395.

[11] G. Mani, S. Kim, and K. Kim, Development of folate-thioglycolate-gold nanoconjugates by using citric acid-peg branched polymer for inhibition of MCF-7 cancer cell proliferation. *Biomacromolecules*, 19(8): 3257-3267.

[12] E. Albiter, M.A. Valenzuela, S. Alfaro, et al., Photocatalytic deposition of Ag nanoparticles on TiO 2: Metal precursor effect on the structural and photoactivity properties. *Journal of Saudi Chemical Society*, 2015, 19(5): 563-673.

[13] K. Khanra, S. Panja, I. Choudhuri, et al., Antimicrobial and cytotoxicity effect of silver nanoparticle synthesized by *Croton bonplandianum* Baill. leaves. *Nanomedicine Journal*, 2016, 3(1): 15-22.

[14] M. El-Kemary, Y. Abdel-Moneam, M. Madkour, et al., Enhanced photocatalytic degradation of Safranin-O

by heterogeneous nanoparticles for environmental applications. *Journal of Luminescence*, 2011, 131(4): 570-576.
[15] M. Oves, M. Arshad, M.S. Khan, et al., Anti-microbial activity of cobalt doped zinc oxide nanoparticles: Targeting water borne bacteria. *Journal of Saudi Chemical Society,* 2015, 19(5): 581-588.
[16] S. Ahmed, M. Ahmad, B.L. Swami, et al., A review on plants extract mediated synthesis of silver nanoparticles for antimicrobial applications: A green expertise. *Journal of advanced research*, 2016, 7(1): 17-28.
[17] P. Mukherjee, A. Ahmad, D. Mandal, et al., Fungus-mediated synthesis of silver nanoparticles and their immobilization in the mycelial matrix: A novel biological approach to nanoparticle synthesis. *Nano Letters*, 2001, 1(10): 515-519.
[18] S. Shivaji, S. Madhu, and S. Singh, Extracellular synthesis of antibacterial silver nanoparticles using psychrophilic bacteria. *Process Biochemistry*, 2011, 46(9): 1800-1807.
[19] S. Rajeshkumar, C. Malarkodi, K. Paulkumar, et al., Algae mediated green fabrication of silver nanoparticles and examination of its antifungal activity against clinical pathogens. *International Journal of Metals*, 2014, 2014: 1-8.
[20] G.K. Devi, P.S. Kumar, and KS. Kumar, Green synthesis of novel silver nanocomposite hydrogel based on sodium alginate as an efficient biosorbent for the dye wastewater treatment: Prediction of isotherm and kinetic parameters. *Desalination and Water Treatment*, 2016, 57(57): 27686-27699.
[21] A.M. Awwad, N.M. Salem, Q.M. Ibrahim, et al., Phytochemical fabrication and characterization of silver/silver chloride nanoparticles using Albizia julibrissin flowers extract. *Adv Mater Lett*, 2015, 6: 726-730.
[22] P. Yugandhar, N. Savithramma, Leaf assisted green synthesis of silver nanoparticles from Syzygium alternifolium (Wt.) Walp. Characterization and Antimicrobial Studies. *Nano Biomed. Eng*, 2015, 7(2): 29-37.
[23] C.M.K.Kumar, P. Yugandhar, and N. Savithramma, Adansoniadigitata leaf extract mediated synthesis of silver nanoparticles; Characterization and antimicrobial studies. *Journal of Applied Pharmaceutical Science,* 2015, 5(08): 82-89.
[24] G. Gnanajobitha, K. Paulkumar, M. Vanaja, et al., Fruit-mediated synthesis of silver nanoparticles using Vitisvinifera and evaluation of their antimicrobial efficacy. *Journal of Nanostructure in Chemistry*, 2013, 3(67): 1-6.
[25] S.O. Adio, C. Basheer, K. Zafarullah et al., Biogenic synthesis of silver nanoparticles; study of the effect of physicochemical parameters and application as nanosensor in the colorimetric detection of Hg^{2+} in water. *International Journal of Environmental Analytical Chemistry,* 2016, 96(8): 776-788.
[26] A. Toobaie, J.W. Kim, I.J. Dolinsek, et al., Diel activity patterns of the fish community in a temperate stream. *Journal of Fish Biology*, 2013, 82(5): 1700-1707.
[27] P.K. Das, A.K. Mondal, A report to the rare and endangered medicinal plants resources in the dry deciduous forest areas of Paschim Medinipur District, West Bengal, India. *International Journal of Drug Discovery and Herbal Research,* 2012, 2(2): 418-429.
[28] K. Khanra, S. Panj, I. Choudhuri et al., Evaluation of Antibacterial Activity and Cytotoxicity of Green Synthesized Silver Nanoparticles Using Scopariadulcis. *Nano Biomed. Eng*, 2015, 7(3): 128-133.
[29] A. Verma, M.S. Mehata, Controllable synthesis of silver nanoparticles using Neem leaves and their antimicrobial activity. *Journal of Radiation Research and Applied Sciences*. 2016, 9(1): 109-915.
[30] D. Jain, H.K. Daima, S. Kachhwaha, et al, Synthesis of plant-mediated silver nanoparticles using papaya fruit extract and evaluation of their anti microbial activities. *Digest Journal of Nanomaterials and Biostructures,* 2009, 4(3): 557-563.
[31] G. Von White, P. Kerscher, R.M. Brown, et al., Green synthesis of robust, biocompatible silver nanoparticles using garlic extract. *Journal of Nanomaterials*, 2012, 2012: 1-12.
[32] K Khanra, S. Panja, I. Choudhuri, et al., Bactericidal and cytotoxic properties of silver nanoparticle synthesized from root extract of Asparagus racemosus. *Nano Biomed. Eng*, 2016, 8(1): 39-46.
[33] S. Panja, I. Chaudhuri, K. Khanra, et al., Biological application of green silver nanoparticle synthesized from leaf extract of RauvolfiaserpentinaBenth. *Asian Pacific Journal of Tropical Disease,* 2016, 6(7): 549-556.
[34] H.M. Ibrahim, Green synthesis and characterization of silver nanoparticles using banana peel extract and their antimicrobial activity against representative microorganisms. *Journal of Radiation Research and Applied Sciences*, 2015, 8(3): 265-275.
[35] S. Ahmed, M. Ahmad, B.L. Swami, et al., Green synthesis of silver nanoparticles using Azadirachtaindica aqueous leaf extract. *Journal of Radiation Research and Applied Sciences*, 2016, 9(1): 1-7.
[36] K. Singh, M. Panghal, S. Kadyan, et al., Green silver nanoparticles of Phyllanthusamarus: as an antibacterial agent against multi drug resistant clinical isolates of Pseudomonas aeruginosa. *Journal of Nanobiotechnology,* 2014, 12(40): 1-9.
[37] K. Anandalakshmi, J. Venugobal, and V. Ramasamy, Characterization of silver nanoparticles by green synthesis method using Pedalium murex leaf extract and their antibacterial activity. *Applied Nanoscience*, 2016, 6(3): 399-408.
[38] J. Umashankari, D. Inbakandan, T.T. Ajithkumar, et al., Mangrove plant, Rhizophora mucronata (Lamk, 1804) mediated one pot green synthesis of silver nanoparticles and its antibacterial activity against aquatic pathogens. *Aquatic Biosystems,* 2012, 8(11): 1-7.
[39] D. Dhanasekaran, R. Thangaraj, Evaluation of larvicidal activity of biogenic nanoparticles against filariasis causing Culex mosquito vector. *Asian Pacific Journal of Tropical Disease*, 2013, 3(3): 174-179.
[40] C. Kamaraj, A. Bagavan, G. Elango, et al., Larvicidal activity of medicinal plant extracts against Anopheles subpictus & Culextritaeniorhynchus. *The Indian Journal of Medical Research*, 2011, 134(1): 101-106.
[41] S. Tennyson, K.J. Ravindran, and S. Arivoli, Screening of twenty five plant extracts for larvicidal activity against Culex quinquefasciatus Say (Diptera: Culicidae). *Asian Pacific Journal of Tropical Biomedicine*, 2012, 2(2): S1130-S1134.
[42] K. Roy, C.K. Sarkar, and C.K. Ghosh, Photocatalytic activity of biogenic silver nanoparticles synthesized using yeast (Saccharomyces cerevisiae) extract. *Applied Nanoscience*, 2015, 5(8): 953-959.
[43] M. Vanaja, K. Paulkumar, M. Baburaja, et al., Degradation of methylene blue using biologically synthesized silver nanoparticles. *Bioinorganic Chemistry and Applications*, 2014, 2014: 1-8.
[44] P. Mulvaney, Surface plasmon spectroscopy of nanosized metal particles. *Langmuir*, 1996, 12(3): 788-800.
[45] K. Paulkumar, G. Gnanajobitha, M. Vanaja, et al., Piper nigrum leaf and stem assisted green synthesis of silver nanoparticles and evaluation of its antibacterial activity against agricultural plant pathogens. *Scientific World Journal*, 2014, 2014: 1-9.
[46] J.A.J. Paul, B.K. Selvi, and N. Karmegam, Biosynthesis

of silver nanoparticles from *Premnaserratifolia L*. leaf and its anticancer activity in CCl4- induced hepato-cancerous Swiss albino mice. *Appl Nanosci*, 2015, 5(8): 937-944.
[47] G.W. Lu, P. Gao, *Emulsions and microemulsions for topical and transdermal drug delivery in Handbook of non-invasive drug delivery systems*. William Andrew Publishing, 2010: 59-94.
[48] D.L. Denlinger, P.A. Armbruster, *Molecular physiology of mosquito diapause in Advances in Insect Physiology.* Academic Press, 2016: 329-361.
[49] M. Ahmed, K. Jamil, Cytotoxicity of neoplastic drugs Gefitinib, Cisplatin, 5-FU, Gemcitabine, and Vinorelbine on human cervical cancer cells (HeLa). *Biology and Medicine*, 2011, 3(5): 60-71.
[50] C.W. Yde, M. Gyrd-Hansen, A.E. Lykkesfeldt, et al., Breast cancer cells with acquired antiestrogen resistance are sensitized to cisplatin-induced cell death. *Molecular Cancer Therapeutics*, 2007, 6(6): 1869-1876.